

# Catalytic Combustion of Methane on $\text{La}_{2-x}\text{Sr}_x\text{NiO}_{4-\lambda}$ ( $x = 0.00\text{--}1.50$ ) Perovskites prepared *via* the Nitrate and Citrate Routes

Athanasios K. Ladavos and Philip J. Pomonis\*

Department of Chemistry, University of Ioannina, Ioannina 45332, Greece

The catalytic combustion of  $\text{CH}_4$  with stoichiometric amounts of oxygen to  $\text{CO}_2$  and  $\text{H}_2\text{O}$  has been studied over two series of perovskite solids  $\text{La}_{2-x}\text{Sr}_x\text{NiO}_{4-\lambda}$  ( $x = 0.00, 0.25, 0.50, 0.75, 1.00, 1.25, 1.50$ ) prepared *via* the nitrate and citrate methods. The reaction rate consists of two rate components, one suprafacial employing oxygen from the gas phase and active at low temperatures and another intrafacial, employing oxygen from the perovskite lattice and apparent mainly at high temperatures. The reaction is first order relative to  $\text{CH}_4$  for the two series and over the whole range of reaction temperature. The reaction order for oxygen decreases from 0.5 to 0.2 as the temperature increases. The Arrhenius-type temperature dependence of the reaction rate for the suprafacial and the intrafacial process have been determined for the  $\text{La}_{1.25}\text{Sr}_{0.75}\text{NiO}_4$  samples to be 47.4 and 110.8  $\text{kJ mol}^{-1}$  for the nitrate solid and 61.5 and 52.5  $\text{kJ mol}^{-1}$  for the citrate solid, showing that the oxygen is much more strongly bound on the catalyst of nitrate origin. The catalytic activity of both series is uniquely related to  $\% \text{Ni}^{3+}$  in the perovskite.

Catalytic combustion of hydrocarbons is of great interest because it offers advantages over conventional flame combustion. Large amounts of nitrogen oxides are produced during conventional combustion in air atmosphere at temperatures up to 1300 °C. The formation of  $\text{NO}_x$  can be diminished by using active catalysts at lower temperatures. There are two special requirements of a candidate catalytic material for combustion: (i) thermal and chemical stability; and (ii) catalytically active phases in the high-temperature, highly oxidizing combustion environment.<sup>1,2</sup> The catalysts with the greatest specific combustion activity at low temperature are the supported noble metals. However, the noble metals are expensive, susceptible to sintering and they tend to form volatile oxides in the presence of oxygen at high temperature.<sup>3</sup> Moreover, all metals and most simple oxides such as  $\text{Co}_3\text{O}_4$  are volatile and sinter easily at such elevated temperatures. Complex metal oxides may have optimal properties for catalytic combustion because they combine stable, low-volatility oxides such as lanthanide (rare-earth) oxides with metals or metal oxides of high catalytic activity such as platinum, cobalt oxide, nickel oxide.

Libby<sup>4</sup> and Pedersen and Libby<sup>5</sup> were the first investigators to suggest the potential application of perovskites as oxidation catalysts. Perovskites have been examined in detail with respect to CO oxidation for application in exhaust gas clean-up<sup>6–8</sup> and combustion of light hydrocarbons.<sup>9–11</sup> However, little is known about the specific activities of the perovskites for the total oxidation of methane.<sup>12</sup> In the present work the particular behaviour of these materials and especially of perovskites  $\text{La}_{2-x}\text{Sr}_x\text{NiO}_{4-\lambda}$  is investigated in terms of the relative ease with which oxygen species can be released from the catalyst surface. Voorhoeve<sup>13</sup> has proposed that the oxidation over perovskite oxides proceeds by both suprafacial and intrafacial reactions. In the suprafacial process the reaction rate appears to be correlated primarily with the electronic configurations of the surface transition-metal ions or the surface defects. In this case the reaction takes place between the adsorbed species on the surface at relatively low temperatures. Conversely, the intrafacial mechanism takes over at high temperatures and the reaction rate appears to be correlated primarily with the thermodynamic stability of oxygen vacancies adjacent to a transition-metal ion. The aim of this study is to examine the mechanisms, both suprafacial and intrafacial, of methane oxidation over the  $\text{La}_{2-x}\text{Sr}_x\text{NiO}_{4-\lambda}$  ( $x = 0.00\text{--}1.50$ ) perovskite

solids prepared by the nitrate and citrate methods and compare the behaviour of these materials.

## Experimental

### Methods of Catalyst Preparation and Characterization

Two series of catalysts with the general formulae  $\text{La}_{2-x}\text{Sr}_x\text{NiO}_4$ , where  $x = 0.00, 0.25, 0.50, 0.75, 1.00, 1.25$  and 1.50, were prepared, according to the nitrate<sup>14</sup> and the citrate<sup>15</sup> methods. Details of the methods of preparation are given in ref. 16. Briefly, in the nitrate method the corresponding nitrate salts were mixed and heated slowly to 600 °C, followed by grinding and heating for 4 h at 1050 °C under atmospheric conditions. In the citrate method the calculated amounts of nitrate salts were dissolved in a small amount of water and an amount of citric acid, sufficient to replace all the nitrate groups by citrate groups, was added. The mixtures were next dried by heating for 24 h at 105 °C and a nearly solidified gel was obtained. This was heated slowly to 350 °C for 1 h to decompose the nitrate and subsequently at 600, 700, 800, 900 and 1050 °C. At each temperature the X-ray diffraction (XRD) patterns of the solids were examined. The prepared solids, together with some of their typical properties, are listed in Table 1.

The XRD patterns of the prepared solids were obtained using a Philips system (PW 2253 lamp, PW 1050 goniometer, PW 1965/50 analogue detector using  $\text{Co-K}\alpha$  radiation ( $\lambda = 1.7902 \text{ \AA}$ )). Details of the corresponding XRD patterns are included in ref. 16. The samples employed in the present study are those of the nitrate solids in which pure perovskite phase was identified after firing at 1050 °C and the citrate solids in which perovskite was identified after heating at 800 or 900 °C, depending on the solid.<sup>16</sup>

The specific surface areas (s.s.a.) of the solids were measured by the BET single-point method using a Carlo-Erba Sorptory 1750 apparatus. The values found are listed in Table 1. In order to diminish the error of the single-point method, which employs an automatic system, we prepared a rather large amount of solid (*ca.* 10 g), especially for the nitrate solids which have s.s.a. *ca.* 1–2  $\text{m}^2 \text{ g}^{-1}$ .

The  $\text{Ni}^{3+}$  content of the samples was determined iodometrically according to the method described in ref. 17, specific details of the method are also in ref. 16. The results are included in Table 1. An exact knowledge of the stoichiometry

Table 1 Characteristics of the samples

sample	method of preparation	$\lambda$	final firing temp./°C	s.s.a./m <sup>2</sup> g <sup>-1</sup>	Ni <sup>3+</sup> (%)	$\mu_{\text{eff}}$ ( $\mu_{\text{B}}$ )
La <sub>2</sub> NiO <sub>4-<math>\lambda</math></sub>	{ nit	-0.13	1050	0.60	26	1.79
	{ cit	-0.15	900	1.90	30	1.70
La <sub>1.75</sub> Sr <sub>0.25</sub> NiO <sub>4-<math>\lambda</math></sub>	{ nit	-0.045	1050	1.76	34	1.63
	{ cit	-0.075	800	4.90	40	1.60
La <sub>1.50</sub> Sr <sub>0.50</sub> NiO <sub>4-<math>\lambda</math></sub>	{ nit	0.025	1050	1.76	45	1.61
	{ cit	0.03	800	5.50	44	1.45
La <sub>1.25</sub> Sr <sub>0.75</sub> NiO <sub>4-<math>\lambda</math></sub>	{ nit	0.075	1050	1.55	60	1.48
	{ cit	0.1	800	4.20	55	1.34
LaSrNiO <sub>4-<math>\lambda</math></sub>	{ nit	0.095	1050	1.16	81	1.32
	{ cit	0.235	800	2.50	53	1.36
La <sub>0.75</sub> Sr <sub>1.25</sub> NiO <sub>4-<math>\lambda</math></sub>	{ nit	0.125	1050	0.53	100	1.18
	{ cit	0.42	900	1.30	41	1.45
La <sub>0.50</sub> Sr <sub>1.50</sub> NiO <sub>4-<math>\lambda</math></sub>	{ nit	0.255	1050	0.32	99	1.05
	{ cit	0.505	900	1.30	49	3.22

of the solids enables calculation of the excess, or deficiency,  $\lambda$ , of oxygen in the formulae La<sub>2-x</sub>Sr<sub>x</sub>NiO<sub>4- $\lambda$</sub> . These values are listed in Table 1.

The magnetic susceptibility  $\chi_m$  of the prepared solids was measured at 291 K (room temperature) in a Cahn-Ventron DM-2 magnetic balance according to the Faraday method. From the values of  $\chi_m$ , after correction for diamagnetic contributions,  $\chi_{\text{corr}}$ , the effective magnetic moments  $\mu_{\text{eff}}$  (in  $\mu_{\text{B}}$ ) were calculated *via* the well known relationship  $\mu_{\text{eff}} = 2.48(\chi_{\text{corr}} T)^{1/2}$ . These are also included in Table 1.

#### CH<sub>4</sub> Combustion

The methane combustion was carried out in a bench-scale plug-flow reactor (PFR) connected to a gas chromatograph (GC) for analysis. A mixture of CH<sub>4</sub>:O<sub>2</sub>:He = 1:2:20, total flow rate 115 cm<sup>3</sup> min<sup>-1</sup> was passed through the catalyst bed containing 0.5 g of catalyst. Analyses of the reactants and products were carried out by sampling 1 cm<sup>3</sup> of the gases to a Shimadzu 15A GC equipped with a TCD with He as carrier gas and connected to a Chromatopak C-R6A integrator system. The column used for analysis was a Porapak Q (stainless steel, 2 m long and 0.317 × 10<sup>-2</sup> m internal diameter) using the following temperature programme: 30 °C for 3 min then the temperature was increased at 30 °C min<sup>-1</sup> to 150 °C, then held at 150 °C for 3 min. During the first 3 min O<sub>2</sub>, CH<sub>4</sub> and CO<sub>2</sub> are eluted from the column into the detector. Then, at elevated temperature, the flowing gas elutes the product H<sub>2</sub>O from the column. The carrier-gas flow was kept at 17.5 cm<sup>3</sup> min<sup>-1</sup> and the products line from the exit of the reactor to the injector port was kept at 100 °C to avoid condensation of the H<sub>2</sub>O. The catalysts were active between 500 and 740 °C. The experiments took place at 20 °C intervals chosen randomly. In each experiment the reaction rate was calculated as the amount (mol) reacted per unit time and unit mass or surface area. The results for three typical reaction temperatures are shown in Fig. 1 for the nitrate and citrate samples.

#### Results

The final firing temperature indicated in Table 1 corresponds to that at which the pure perovskite phase was first observed free of admixtures as shown by the XRD patterns. Note that in the samples La<sub>0.75</sub>Sr<sub>1.25</sub>NiO<sub>4</sub> and La<sub>0.5</sub>Sr<sub>1.5</sub>NiO<sub>4</sub> some traces of NiO were detectable with difficulty in the XRD patterns.

As can be seen from Table 1, the s.s.a. of the samples prepared by the citrate method are on average three times larger than the nitrate samples. Note the desintering action of Sr,

which nevertheless is apparent up to a certain degree ( $x = 0.50$ ) of substitution of La by Sr. Thereafter the s.s.a. drops.

The gradual substitution of La<sup>3+</sup> by Sr<sup>2+</sup> causes oxidation of an increasing amount of Ni<sup>2+</sup> to Ni<sup>3+</sup>. This transformation seems to proceed identically for the two series of solids up to  $x = 0.75$ . From  $x = 0.75$  to  $x = 1.50$  the nitrate samples show a continuously increasing percentage of Ni<sup>3+</sup> and at  $x = 1.25$  and 1.50 all the nickel appears to be in the +3 valence state. Conversely, in the citrate samples the percentage of Ni<sup>3+</sup> never exceeds 55%. This is probably due to the reducing action at residual carbon in the samples prepared by the citrate method which prevents further oxidation of nickel.

The magnetic moments at room temperature of the nitrate solids (Table 1) decrease normally as  $x$  increases from 0.00 to 1.50. This decrease is explained by the transformation of

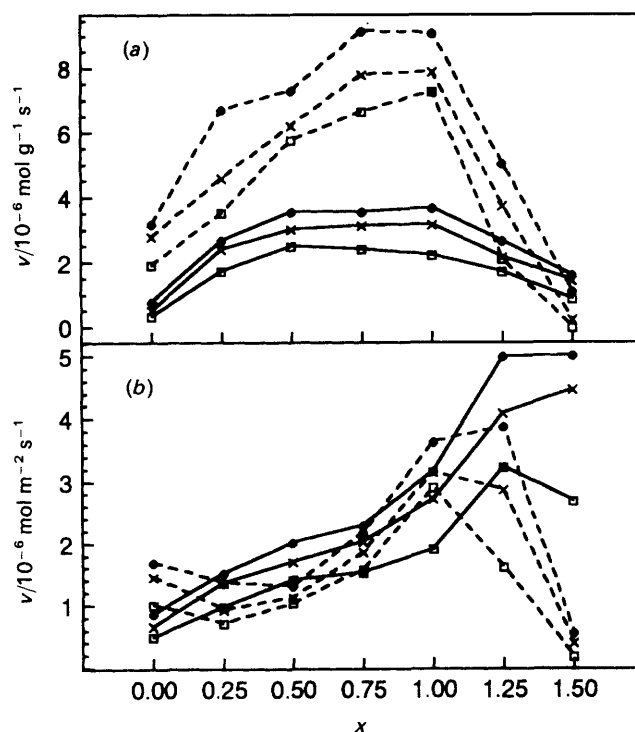


Fig. 1 Reaction rates calculated as (a) mol g<sup>-1</sup> s<sup>-1</sup> and (b) mol m<sup>-2</sup> s<sup>-1</sup> for the CH<sub>4</sub> combustion over the nitrate (—) and citrate (---) La<sub>2-x</sub>Sr<sub>x</sub>NiO<sub>4- $\lambda$</sub>  samples as a function of  $x$ . Reaction rates were measured at □, 580; ×, 600 and ●, 620 °C

$\text{Ni}^{2+}$  ( $d^8$ ), which has two unpaired electrons, to  $\text{Ni}^{3+}$  ( $d^7$ ), which in a strong octahedral crystal field has only one unpaired electron. Note that a weak field would result in a higher number of unpaired electrons and therefore higher  $\mu_{\text{eff}}$  values. The citrate solids show a normal magnetic moment increase up to  $x = 0.75$ . From  $x = 0.75$  to 1.25,  $\mu_{\text{eff}}$  remains practically constant, indicating smaller changes in the number of unpaired electrons, as indeed found by the previous experiments related to the oxidation state of nickel. The large value of  $\mu_{\text{eff}}$  at  $x = 1.50$  for the citrate sample is probably due either to some other unidentified crystal structure or to an altered degree of oxidation.

The catalytic activity of the solids is shown in Fig. 1 in the form of the rate  $v$  of  $\text{CH}_4$  oxidation calculated either per unit mass ( $v/\text{mol g}^{-1} \text{s}^{-1}$ ) or per unit area ( $v/\text{mol m}^{-2} \text{s}^{-1}$ ) of the catalysts as a function of the degree of substitution of La by Sr.

### Discussion

As shown in Fig. 1 the catalytic activity calculated per unit mass is higher for the citrate samples than the nitrate samples, except for the sample with  $x = 1.50$  where the opposite is true. Moreover, substitution of La by Sr increases the activity for both series of solids up to  $x = 0.75$ –1.00 and thereafter decreases it. However, if the activity is calculated per unit area then it appears to increase with  $x$  for the whole range of substitution for the nitrate samples. In contrast, the activity for the citrate samples seems to be almost constant up to  $x = 0.50$ , increases from  $x = 0.50$  to 1.00 then with further substitution of La by Sr decreases.

Fig. 2 shows a comparison of the rates observed for the two series of solids, both per unit mass and per unit surface area. It is clear that the reaction rate on citrate samples, if calculated per unit mass, is on average three times higher than that on nitrate ones. The reaction rate per unit surface area shows that the activity for the citrate samples is about the same as for the nitrate samples. This demonstrates the fact that the higher surface area of the citrate samples, on average three times larger than that of the nitrate solids, is the main reason for the difference in the catalytic activity. The case of  $x = 1.50$  [see Fig. 2(b)] does not follow this pattern. As noted previously it corresponds to abnormal magnetic behaviour, indicating a different electronic configuration or a structure modification.

In order to determine the kinetic parameters and the activation energies of the reaction we checked initially to see if the behaviour of the system obeys the following equations:

$$\text{Model I: } v = kP_{\text{CH}_4}P_{\text{O}_2} \quad (1)$$

$$\text{Model II: } v = kP_{\text{CH}_4}/P_{\text{O}_2} \quad (2)$$

$$\text{Model III: } v = kP_{\text{O}_2} \quad (3)$$

where  $P_{\text{CH}_4}$  and  $P_{\text{O}_2}$  are the partial pressures of methane and oxygen. Eqn. (1)–(3) were then substituted in the equation for the plug-flow reactor:

$$F dX = v dS \quad (4)$$

where  $F$  is the mass flow rate of  $\text{CH}_4$  and  $S$  denotes the surface area of the catalyst used. Eqn. (1)–(3) correspond to weak adsorption of reactants and products, to weak adsorption of methane and strong adsorption of oxygen and to reaction of methane with strongly adsorbed oxygen on the catalyst surface, respectively. After integration and taking

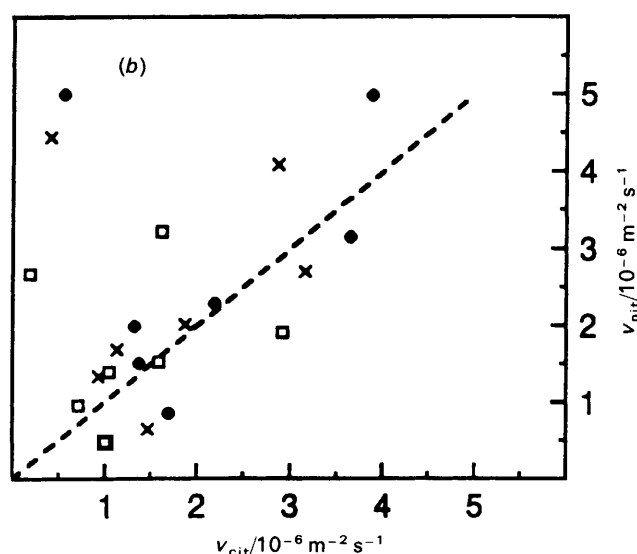
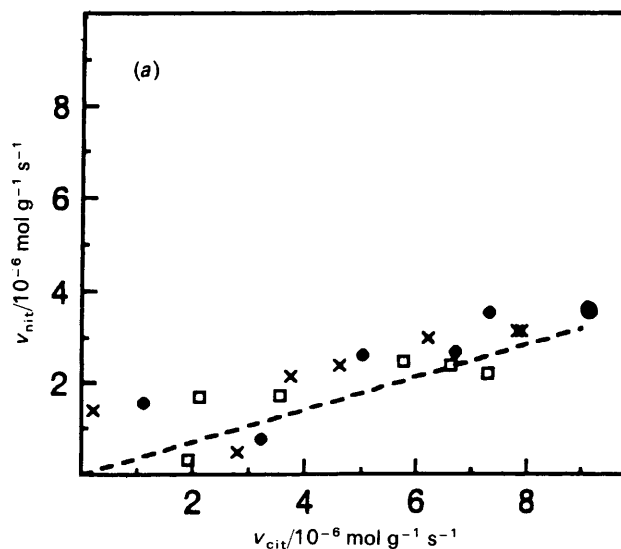


Fig. 2 Comparison of the rates of  $\text{CH}_4$  combustion calculated as (a)  $\text{mol g}^{-1} \text{s}^{-1}$  and (b)  $\text{mol m}^{-2} \text{s}^{-1}$  over the nitrate and citrate samples. The dashed lines are drawn according to relationships (a)  $v_{\text{nit}} = \frac{1}{3}v_{\text{cit}}$  for the comparison of rates per unit mass and (b)  $v_{\text{nit}} = v_{\text{cit}}$  for the comparison per unit area. Symbols as in Fig. 1

into account the experimental conditions followed by taking logarithms of the equations obtained we finally obtain:

$$\text{Model I: } \ln[X/(1-X)] = \ln[2(P_t)^2/529F] + \ln S + \ln A - E/RT \quad (5)$$

$$\text{Model II: } \ln X = \ln(S/2F) + \ln A - E/RT \quad (6)$$

$$\text{Model III: } \ln[-\ln(1-X)] = \ln(P_t/23F) + \ln S + \ln A - E/RT \quad (7)$$

where  $X$  is the degree of methane conversion and  $P_t = 1 \text{ atm}^\dagger$  is the total pressure. Eqn. (5)–(7) in the form:

$$\ln[f(X)] = f(10^3/T) \quad (8)$$

where  $\ln[f(X)]$  is the left-hand side of eqn. (5)–(7), were tested statistically in order to select the line with the best

$^\dagger 1 \text{ atm} = 101325 \text{ Pa}$ .

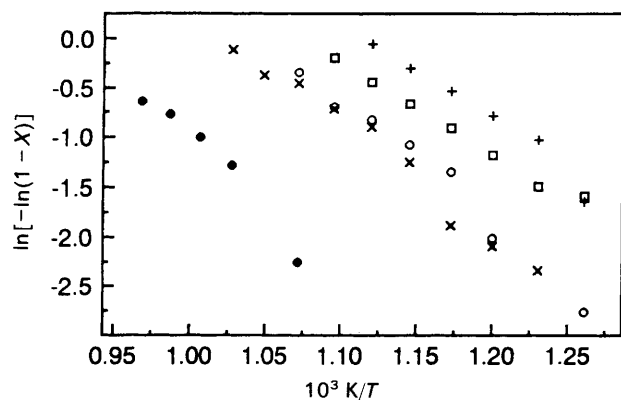


**Fig. 3** Arrhenius plots for the  $\text{CH}_4$  combustion according to eqn. (7) for typical nitrate ( $\square$ ,  $\text{La}_{1.25}\text{Sr}_{0.75}\text{NiO}_4$ ;  $\circ$ ,  $\text{La}_{0.75}\text{Sr}_{1.25}\text{NiO}_4$ ) or citrate samples ( $+$ ,  $\text{La}_{1.25}\text{Sr}_{0.75}\text{NiO}_4$ ;  $\times$ ,  $\text{La}_{0.75}\text{Sr}_{1.25}\text{NiO}_4$  and  $\bullet$ ,  $\text{La}_{0.5}\text{Sr}_{1.5}\text{NiO}_4$ )

correlation coefficient and the smallest standard deviation which would represent the kinetic model describing our experiments. This procedure was similar to the one used previously in similar cases.<sup>16,18–20</sup> However, no straight Arrhenius-type lines were observed in any of the cases examined. An example is shown in Fig. 3 for the Model III, similar discrepancies were observed for the other models.

Furthermore attempts to distinguish two slopes at every line were unsuccessful. Therefore we were led to the conclusion that, as in other similar cases describing the behaviour of hydrocarbon combustion,<sup>2,12</sup> the oxidation of CO by oxygen<sup>6</sup> or the reduction of NO by CO<sup>6</sup> on similar solids, there are two different reaction mechanisms which operate at different temperatures. In such cases an exact temperature at which the mechanism changes does not exist and the change is rather gradual. Thus a more detailed investigation of the kinetics of methane oxidation was carried out by varying the partial pressures of oxygen and methane. The results were expressed by the empirical rate equation

$$v = k(P_{\text{CH}_4})^m(P_{\text{O}_2})^n \quad (9)$$

where  $m$  and  $n$  are the orders of reaction with respect to methane and oxygen. As test materials,  $\text{La}_{1.25}\text{Sr}_{0.75}\text{NiO}_4$  samples, prepared by the nitrate and citrate methods, were used at three different reaction temperatures. Then using plots of the form  $\log v = f(\log P_i)_{P_j=\text{constant}}$ , where  $i = \text{CH}_4$  or  $\text{O}_2$  and  $j = \text{O}_2$  or  $\text{CH}_4$ , respectively, the values of  $m$  and  $n$  were easily calculated. The results at every temperature and the corresponding correlation coefficients ( $c$ ) are shown in Table 2.

As can be seen from Table 2 the reaction order for  $\text{CH}_4$  is unity, or nearly unity, for the two solids over the whole range of reaction temperature. However, the corresponding reaction order for oxygen decreases from *ca.* 0.5 at low temperature (450 °C) to 0.2 at 600 °C. These results are very close to those of Arai *et al.*<sup>12</sup> who studied the perovskites  $\text{La}_{0.8}\text{Sr}_{0.2}\text{MO}_3$  (where  $M = \text{Mn}$  and  $\text{Co}$ ) for the same reaction. These results indicate that there are probably two sources of oxygen participating in the process with unequal

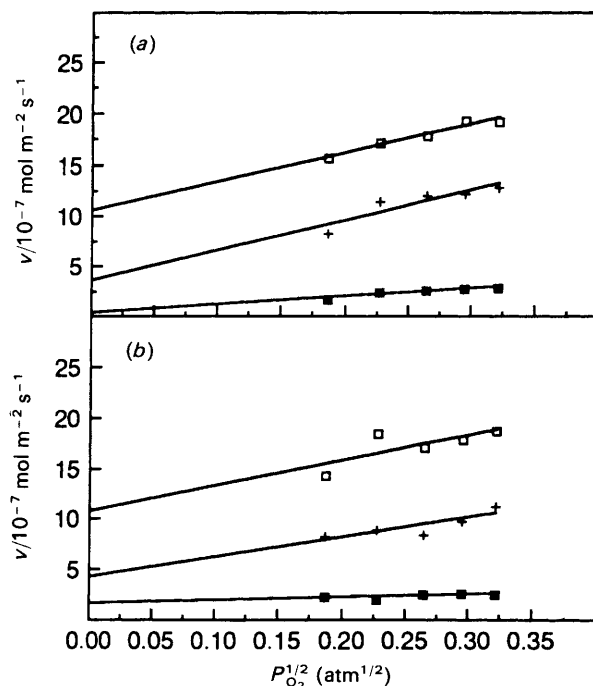


**Fig. 4** Dependence of reaction rate  $v$  ( $\text{mol m}^{-2} \text{s}^{-1}$ ) on the square root of oxygen pressure, over  $\text{La}_{1.25}\text{Sr}_{0.75}\text{NiO}_4$  prepared by (a) the nitrate and (b) the citrate method at three temperatures:  $\blacksquare$ , 450;  $+$ , 550;  $\square$ , 600 °C

and variable contributions in the low- and high-temperature reaction region.<sup>2,10,12</sup>

The contribution of each of these two oxygen sources to methane oxidation at a specific temperature is deduced from the plot of the reaction rate *vs.* the square root of oxygen partial pressure (Fig. 4).

As is shown in Fig. 4 the reaction rate at 450 °C for an oxygen partial pressure approaching zero, is nearly zero. A gradual increase in the reaction rate is observed with increase in reaction temperature up to 600 °C. This result indicates that there is a source of oxygen which causes reaction even in the absence of oxygen in the gas phase. The slope of the lines in Fig. 4 corresponds to the gas-phase oxygen contribution while the intercept represents the contribution of lattice oxygen to the reaction rate.

Thus the kinetic analysis of the reaction can be based on two rate equations, one for low temperatures

$$v_1 = k_1 P_{\text{CH}_4}(P_{\text{O}_2})^{1/2} \quad (10)$$

and one for high temperatures

$$v_2 = k_2 P_{\text{CH}_4} \quad (11)$$

At low reaction temperatures atomic oxygen is adsorbed on the catalyst surface where it reacts with methane molecules adsorbed on the surface, while at high temperature reaction occurs between strongly bound surface oxygen from the oxide lattice and weakly held adsorbed methane molecules.

**Table 2** Orders of reaction with respect to methane ( $m$ ) and oxygen ( $n$ ) and the corresponding correlation coefficient ( $c$ ), at various reaction temperatures

sample	450 °C		550 °C		600 °C	
	$m/c$	$n/c$	$m/c$	$n/c$	$m/c$	$n/c$
$\text{La}_{1.25}\text{Sr}_{0.75}\text{NiO}_4$ (nit)	1.1/0.98	0.44/0.96	1.09/1.00	0.37/0.91	1.06/1.00	0.20/0.98
$\text{La}_{1.25}\text{Sr}_{0.75}\text{NiO}_4$ (cit)	0.84/0.83	0.36/0.88	1.07/0.95	0.24/0.82	0.97/0.97	0.21/0.94

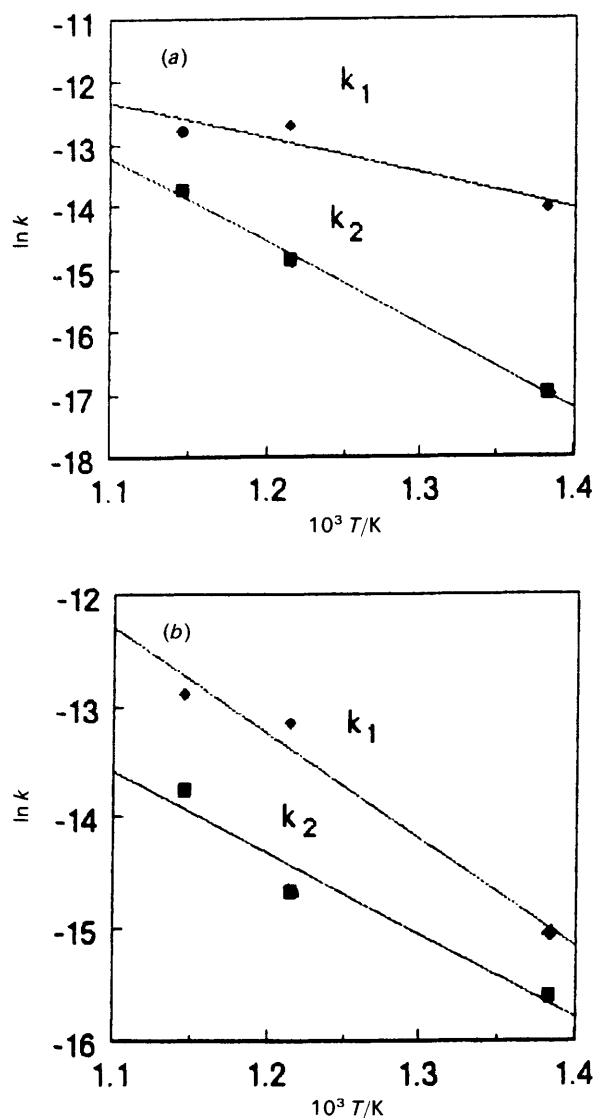


Fig. 5 Arrhenius plots of the rate constants for  $\text{CH}_4$  combustion over  $\text{La}_{1.25}\text{Sr}_{0.75}\text{NiO}_4$  prepared by (a) the nitrate and (b) the citrate methods. For the definition of  $k_1$  and  $k_2$  see text.  $\blacklozenge$ ,  $k_1$  and  $\blacksquare$ ,  $k_2$

Then from Fig. 4 and the equations of the form

$$v_{\text{total}} = v_1 + v_2 = k_1 P_{\text{CH}_4} (P_{\text{O}_2})^{1/2} + k_2 P_{\text{CH}_4} \quad (12)$$

which describe the corresponding lines, the apparent rate constant  $k_1$  can be calculated for  $P_{\text{O}_2}$  decreasing towards zero ( $P_{\text{O}_2} \rightarrow 0$ ) and then the values of  $k_2$  can be easily found. The calculated values of  $k_1$  and  $k_2$  at three different temperatures are included in Table 3.

From the Arrhenius plots (Fig. 5) of the two apparent rate constants  $k_1$  and  $k_2$  we can calculate the activation energies for each of the two mechanisms. Thus for the  $\text{La}_{1.25}\text{Sr}_{0.75}\text{NiO}_4$  sample prepared by the nitrate method the apparent activation energies  $E_1 = 47.4$  and  $E_2 = 110.8$  kJ

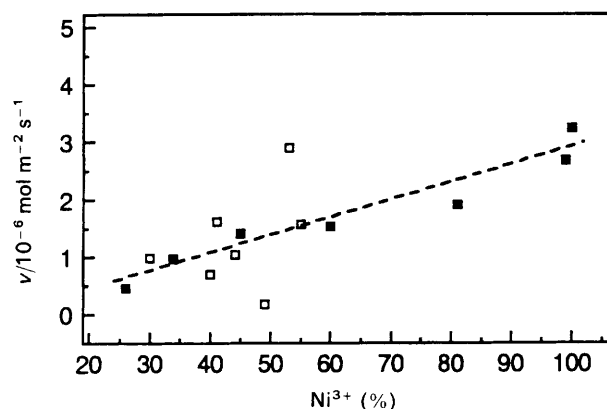


Fig. 6 Dependence of reaction rate  $v$  ( $\text{mol m}^{-2} \text{s}^{-1}$ ) at  $580^\circ\text{C}$  on the percentage of  $\text{Ni}^{3+}$  from Table 1:  $\blacksquare$ , nitrate and  $\square$ , citrate samples

$\text{mol}^{-1}$ , for the reaction with gas-phase oxygen and lattice oxygen, respectively, are obtained. For the sample prepared by the citrate method the corresponding values were  $E_1 = 61.4$  and  $E_2 = 52.5$  kJ  $\text{mol}^{-1}$ , respectively. The above activation energies show that the gas-phase oxygen is more active than the lattice oxygen for oxidation of methane on the nitrate solids. For the citrate solids the two routes are almost equally favoured energetically. An interesting problem is to estimate the temperature of the high-temperature mechanism. Although it seems that in the range of temperature examined in this work both mechanisms participate in the oxidation process, we may estimate the temperature where the ratio  $k_1/k_2$  tends to unity. Thus for the nitrate samples the relationship  $(k_1/k_2) = f(T)$  yields  $(k_1/k_2) = 68.04 - 0.109T$  with a correlation coefficient  $C = 1.00$ . This means that at  $T = 615^\circ\text{C}$  the rate constant  $k_2$  for the high-temperature oxidation exceeds the rate constant  $k_1$  for the low-temperature process. For the citrate solids the plot  $(k_1/k_2) = f(T)$  yields a parabola with two points for  $k_1/k_2 = 1$  at  $T = 441$  and  $617^\circ\text{C}$ . Although the situation here is more complicated either intrinsically or because of some experimental inaccuracies it seems that a switching point should occur probably around  $610\text{--}620^\circ\text{C}$ .

Another interesting feature is the dependence of reaction rate  $v$  ( $\text{mol m}^{-2} \text{s}^{-1}$ ) on the  $\text{Ni}^{3+}$  content of the samples. In Fig. 6 we observe that the reaction rate of a typical reaction temperature ( $580^\circ\text{C}$ ) increases with increase in  $\text{Ni}^{3+}$  content. This observation shows that the higher valence state of nickel is more active than the lower oxidation state for this reaction.

Voorhoeve *et al.*<sup>6</sup> and Tascón and Tejuca<sup>7</sup> studied the influence of cations in site B of various perovskites with the general formulae  $\text{ABO}_3$ , where  $\text{B} = \text{Cr}, \text{Mn}, \text{Fe}$  or  $\text{Co}$ , on the catalytic activity for the CO oxidation. It is known that the octahedral environment on the B ions splits the d orbitals into two levels, the lower ( $t_{2g}$ ) and the higher ( $e_g$ ) levels. They observed that maximum activity is attained for an occupation of the  $e_g$  levels of less than one electron while at the same time the  $t_{2g}$  levels are half-filled or totally filled. In our samples the  $\text{Ni}^{3+}$  ions, as the magnetic measurements have

Table 3 Values of  $k_1$  and  $k_2$  calculated from Fig. 4 and eqn. (12)

$T/^\circ\text{C}$	$\text{La}_{1.25}\text{Sr}_{0.75}\text{NiO}_4$ (nit)		$\text{La}_{1.25}\text{Sr}_{0.75}\text{NiO}_4$ (cit)	
	$k_1/10^{-7} \text{ mol m}^{-2} \text{ s}^{-1} \text{ atm}^{-1.5}$	$k_2/10^{-7} \text{ mol m}^{-2} \text{ s}^{-1} \text{ atm}^{-1}$	$k_1/10^{-7} \text{ mol m}^{-2} \text{ s}^{-1} \text{ atm}^{-1.5}$	$k_2/10^{-7} \text{ mol m}^{-2} \text{ s}^{-1} \text{ atm}^{-1}$
450	8.07	0.43	2.92	1.69
550	30.04	3.61	19.60	4.31
600	27.94	10.65	25.21	10.80

shown, exist in a strong octahedral crystal field and have  $(t_{2g})^6(e_g)^1$  electronic configuration. According to the above-mentioned observation,<sup>6,7</sup> this electronic configuration not only results in higher catalytic activity than with  $Ni^{2+}$  ions, which have a  $(t_{2g})^6(e_g)^2$  electronic configuration, but also quantifies the activity according to the relationship depicted in Fig. 6.

### Conclusions

The catalytic combustion of  $CH_4$  with stoichiometric amounts of oxygen to  $CO_2$  and  $H_2O$  on perovskites  $La_{2-x}Sr_xNiO_{4-\lambda}$  is a two-mechanism process. The first mechanism operates mainly at low reaction temperature and involves the reaction of adsorbed  $CH_4$  and  $O_2$  in a Langmuir–Hinshelwood type bimolecular process. The second mechanism operates mainly at higher temperatures and involves the reaction between adsorbed  $CH_4$  and lattice oxygen in a Mars–Van Krevelen type process. The temperature at which the rate constant for the second (high-temperature) mechanism exceeds the rate constant for the first (low-temperature) mechanism is 610–620 °C. The total reaction rate does not seem to be influenced by the method of preparation of the solids. On the contrary, the factor which seems to control the activity is the existence of  $Ni^{3+}$  in the perovskite matrix. The apparent activation energies for the suprafacial and intrafacial processes are almost similar in the case of citrate solids, whilst for the nitrate solids the activation energy corresponding to the suprafacial route appears decreased, indicating that the gas-phase oxygen is more active than the lattice oxygen for oxidation of methane.

The authors thank one of the referees for his suggestions which contributed to the improvement of this work.

### References

- 1 J. G. McCarty, M. A. Quinlan and H. Wise, *Proceedings of the 9th International Congress on Catalysis*, Chemical Institute of Canada, Calgary, 1988, p. 1818.
- 2 J. G. McCarty and H. Wise, *Catal. Today*, 1990, **8**, 231.
- 3 J. G. McCarty, R. H. Lamoreaux and M. A. Quinlan, *International Gas Research Conference, Tokyo, 1989*, ed. T. L. Cramer, Gas Research Institute, 1989, vol. III, p. 232.
- 4 W. F. Libby, *Science*, 1971, **171**, 499.
- 5 L. A. Pedersen and W. F. Libby, *Science*, 1972, **176**, 1355.
- 6 R. J. H. Voorhoeve, J. P. Remeika and L. E. Trimble, *Ann. N.Y. Acad. Sci.*, 1976, **272**, 3.
- 7 J. M. D. Tascón and L. G. Tejuca, *React. Kinet. Catal. Lett.*, 1980, **15**, 185.
- 8 J. M. D. Tascón, J. L. G. Fierro and L. G. Tejuca, *Z. Phys. Chem. (Wiesbaden)*, 1981, **124**, 249.
- 9 G. Kremenec, J. M. L. Nietto, J. M. D. Tascón and L. G. Tejuca, *J. Chem. Soc., Faraday Trans. 1*, 1985, **81**, 939.
- 10 T. Seiyama, N. Yamazoe and K. Eguchi, *Ind. Eng. Chem., Prod. Res. Dev.*, 1985, **29**, 19.
- 11 T. Nitadori, S. Kurihara and M. Misono, *J. Catal.*, 1986, **98**, 221.
- 12 H. Arai, T. Yamada, K. Eguchi and T. Seiyama, *Appl. Catal.*, 1986, **26**, 265.
- 13 R. J. H. Voorhoeve, in *Advanced Materials in Catalysis*, ed. J. J. Burton and R. L. Garten, Academic Press, New York, 1977, p. 129.
- 14 I. F. Kononyuk, N. G. Surmach and L. V. Makhnach, *Izv. Akad. Nauk., SSSR, Neorg. Mater.*, 1982, **18**, 1222.
- 15 M. S. G. Baythoun and F. R. Sale, *J. Mater. Sci.*, 1982, **17**, 2757.
- 16 A. K. Ladavos and P. J. Pomonis, *J. Chem. Soc., Faraday Trans.*, 1991, **87**, 3291.
- 17 B. E. Gushee, L. Katz and R. Ward, *J. Am. Chem. Soc.*, 1957, **79**, 5601.
- 18 P. Pomonis, Ch. Kordoulis and A. Lykourghiotis, *J. Chem. Soc., Faraday Trans.*, 1990, **86**, 711.
- 19 Ch. Kordoulis, H. Latsios, A. Lykourghiotis and P. Pomonis, *J. Chem. Soc., Faraday Trans.*, 1990, **86**, 185.
- 20 D. Petrakis, P. J. Pomonis and A. T. Sdoukos, *J. Chem. Soc., Faraday Trans. 1*, 1989, **85**, 3173.

Paper 2/01555B; Received 24th March, 1992